SAISA: TOWARDS MULTIMODAL LARGE LANGUAGE MODELS WITH BOTH TRAINING AND INFERENCE EFFICIENCY

Anonymous authors
Paper under double-blind review

ABSTRACT

Multimodal Large Language Models (MLLMs) mainly fall into two architectures, each involving a trade-off between training and inference efficiency: embedding space alignment (*e.g.* LLaVA) is inefficient during inference, while cross-attention space alignment (*e.g.* Flamingo) is inefficient in training. In this paper, we compare these two architectures and identify key factors for building efficient MLLMs. A primary difference between them lies in how attention is applied to visual tokens, particularly in their interactions with each other. To investigate whether attention among visual tokens is necessary, we propose a new self-attention mechanism, NAAViT (**N**o **A**ttention **A**mong **Vi**sual **T**okens), which eliminates this type of attention. Our pilot experiment on LLaVA-1.5 shows that attention among visual tokens is highly redundant. Based on these insights, we introduce SAISA (**S**elf-**A**ttention **I**nput **S**pace **A**lignment), a novel architecture that enhances both training and inference efficiency. SAISA directly aligns visual features with the input spaces of NAAViT self-attention blocks, reducing computational overhead in both self-attention blocks and feed-forward networks (FFNs). Compared with the LLaVA-1.5 architecture, SAISA reduces the inference FLOPs by 66% and the training budget by 26%, while achieving superior performance in terms of accuracy. Comprehensive ablation studies further validate the effectiveness of SAISA across various LLMs and visual encoders. The code and models will be publicly available.

1 INTRODUCTION

Multimodal Large Language Models (MLLMs) OpenAI (2023); Liu et al. (2024a); Bai et al. (2023b); Chen et al. (2023a); Dai et al. (2023) have shown impressive capabilities in understanding and processing visual information. They typically build on pre-trained Large Language Models (LLMs) Achiam et al. (2023); Chiang et al. (2023); Bai et al. (2023a); Touvron et al. (2023b) and align visual features with the LLMs. There are two primary architectures for aligning visual and text modalities: embedding space alignment and cross-attention space alignment. Embedding space alignment, *e.g.* LLaVA Liu et al. (2023; 2024a), introduces a projector to align visual features with the LLM embedding space and feeds the visual and text tokens into the LLM. Cross-attention space alignment, *e.g.* Flamingo Alayrac et al. (2022), inserts cross-attention blocks and aligns visual features with the attention spaces of these blocks.

However, despite the promising performance of these MLLMs, they involve a trade-off between training and inference efficiency. On the one hand, MLLMs with embedding space alignment exhibit training efficiency, since they introduce only a small number of new parameters to the pre-trained LLMs. For example, LLaVA-1.5-7B is trained in 108 GPU hours from Vicuna-7B Chiang et al. (2023). However, this architecture significantly increases the number of input tokens, and the computational costs of self-attention grow quadratically with the number of tokens, leading to inefficiency during inference. On the other hand, MLLMs with cross-attention space alignment achieve inference efficiency, since they do not require unrolling visual tokens, but they are inefficient during training for introducing a large number of new parameters to the pre-trained LLM. In this paper, we take a step towards building MLLMs with efficiency during both training and inference.

In this paper, we first perform a thorough analysis of these two architectures, identifying key factors for building MLLMs with both training and inference efficiency. To optimize training efficiency, the key factor is minimizing the number of new parameters and employing modules in the pre-trained LLMs for interaction between visual and text modalities. For improving inference efficiency, the main focus is reducing the computational costs associated with visual tokens, particularly in attention blocks and feed-forward networks (FFNs). Based on the analysis of these factors, we introduce NAAViT (**N**o **A**ttention **A**mong **Vi**sual **T**okens), as shown in Figure 3, a self-attention mechanism which eliminates attention among visual tokens to enhance efficiency. Since attention among visual tokens contributes significantly to the quadratically growing computational cost in self-attention blocks, we investigate whether this type of attention is truly essential for MLLMs. Our pilot experiment on LLaVA-1.5 demonstrates that NAAViT outperforms the vanilla self-attention, indicating that attention among visual tokens is highly redundant.

Based on the findings above, we introduce SAISA (**S**elf-**A**ttention **I**nput **S**pace **A**lignment), an architecture for MLLMs with efficiency during both training and inference. As illustrated in Figure 2(c), SAISA employs NAAViT blocks for multimodal interaction and directly aligns the visual features with the input spaces of these blocks. SAISA not only reduces the computational overhead of self-attention blocks, but also significantly lowers the computational costs of FFNs by eliminating the need to apply FFNs to visual tokens. We validate its effectiveness on various LLMs and visual encoders. As shown in Figure 1, SAISA outperforms LLaVA-1.5 architecture in terms of performance, training efficiency, and inference efficiency. Using Vicuna-7B-v1.5 Chiang et al. (2023) as LLM and CLIP-ViT-L/14-336 Radford et al. (2021) as visual encoder, SAISA reduces training budget by 26% and inference FLOPs by 66%, while delivering superior performance. Moreover, SAISA is compatible with techniques to reduce the visual token number, *e.g.* resampler Jaegle et al. (2021).

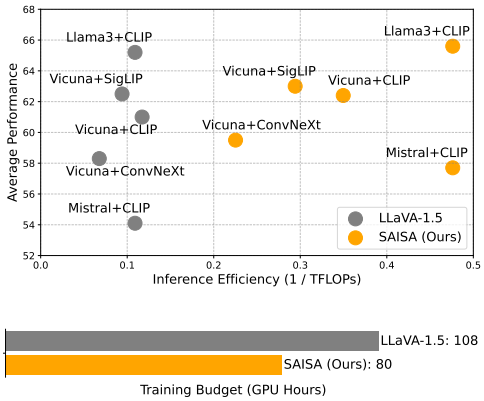

Figure 1: Top: Performance *vs.* inference efficiency based on various LLMs and visual encoders where Average Performance means an average of benchmark scores and inference efficiency is the inverse of inference TFLOPs. Bottom: Training budget comparison where we report the training GPU hours, using Vicuna-7B as LLM and CLIP as visual encoder.

Our contributions are three-fold: (1) Based on our analysis of current MLLM architectures, we propose NAAViT to enhance efficiency of MLLMs, revealing the redundancy of self-attention in MLLMs. (2) We introduce SAISA, an architecture for building MLLMs with both training and inference efficiency by eliminating the computational costs of attention among visual tokens and FFNs on visual tokens. (3) We validate the effectiveness of SAISA across various LLM backbones and visual encoders.

2 Analyzing Current MLLM Architectures

In this section, we analyze the two most common architectures to align visual features with the language model, and summarize key factors for building efficient MLLMs.

Embedding Space Alignment. As illustrated in Figure 2(a), models with this architecture introduce a projector to align visual tokens with the text token embedding space. They concatenate visual tokens and text tokens, and then feed them into the LLM. Notable models with this architecture include LLaVA-1.5 Liu et al. (2024a), Qwen series Bai et al. (2023b; 2025), BLIP series Li et al. (2023c); Dai et al. (2023), and InternVL series Zhu et al. (2025). These models introduce only a small number of new parameters to the pre-trained LLMs, allowing training MLLMs from the LLMs with minimal budget.

However, the concatenated token sequence leads to inference inefficiency. When the number of visual and text tokens is v and t respectively, the computational complexity of self-attention is

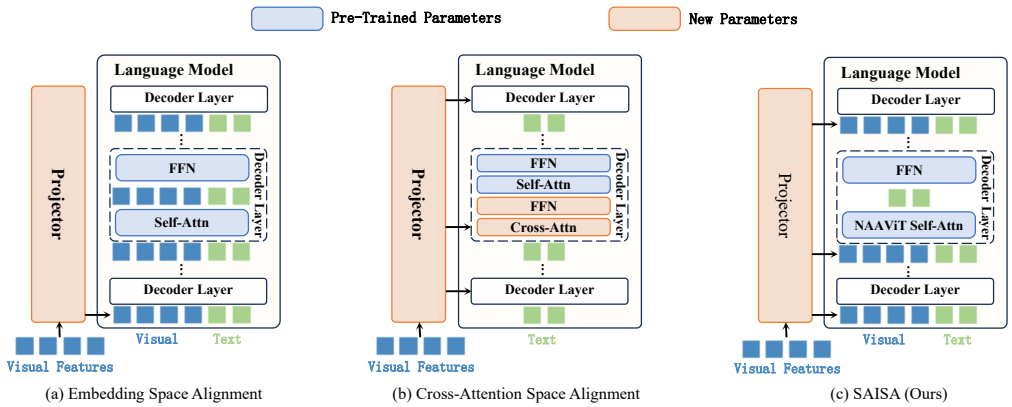

Figure 2: Overview of SAISA and mainstream architectures to align visual features with language models. (a) Aligning visual features with the embedding space of language models is inefficient during inference, *e.g.* LLaVA. (b) Aligning visual features with the attention spaces of new cross-attention blocks is inefficient during training, *e.g.* Flamingo. (c) SAISA aligns visual features with the self-attention input spaces of language models, achieving efficiency during both training and inference.

$\mathcal{O}((v+t)^2)$. It consists of three components, $\mathcal{O}(v^2)$ for attention among visual tokens, $\mathcal{O}(vt)$ for the interaction between text and visual tokens, and $\mathcal{O}(t^2)$ for attention among text tokens. Typically, MLLMs use hundreds or even thousands of visual tokens. For example, LLaVA-1.5 uses 576 visual tokens for a single image, and Sphinx Lin et al. (2023) uses 2,890. In contrast, the number of text tokens is much smaller in most tasks. The average numbers of text tokens in MMMU Yue et al. (2024), POPE Li et al. (2023d) and ScienceQA IMG Lu et al. (2022) are 142, 68, and 210, respectively. As a result, the attention among visual tokens dominates the computational overhead. Moreover, since the FFNs have a large hidden layer dimension, applying FFNs to visual tokens also brings substantial computational costs.

Cross-Attention Space Alignment. As illustrated in Figure 2(b), models with this architecture insert cross-attention blocks and FFNs into the language model, and align visual features with the attention spaces of these cross-attention blocks. Notable models with this architecture include Flamingo Alayrac et al. (2022), OpenFlamingo Awadalla et al. (2023) and Otter Li et al. (2023a). In these models, the attention operation consists of only two components, the interaction between text and visual modalities with complexity $\mathcal{O}(vt)$ in the cross-attention blocks, and the attention among text tokens with complexity $\mathcal{O}(t^2)$ in the self-attention blocks. Compared with embedding space alignment, there is no attention among visual features in the language model. By not executing attention among visual tokens and not applying FFNs to visual tokens, these models are more efficient during inference.

However, the inserted cross-attention blocks and FFNs introduce a large number of new parameters to the pre-trained language model. As a result, training an MLLM with this architecture requires a large amount of data. For example, OpenFlamingo-9B adds 2 billion parameters to Llama-7B Touvron et al. (2023a), and requires training data with 180M samples. In terms of model capabilities, previous work Dai et al. (2024) finds that models utilizing this architecture perform worse than those using embedding space alignment when trained on the same data.

Based on the analyses above, we summarize the key factors for building efficient MLLMs as follows: (1) Reducing the number of new parameters and employing pre-trained modules for multimodal interaction lead to efficiency during training. (2) Reducing computations related to visual tokens, including those in attention blocks and FFNs, leads to efficiency during inference.

3 No Attention Among Visual Tokens

In this section, we propose NAAViT (No Attention Among Visual Tokens) self-attention and perform a pilot experiment to investigate whether attention among visual tokens is necessary for MLLMs.

3.1 PRELIMINARY

Vanilla Self-Attention. In a self-attention block, the input visual-text token sequence is formed as $X = [V, T] \in \mathbb{R}^{(v+t)\times h}$, where $[\cdot, \cdot]$ denotes concatenation along the sequence dimension. To derive the query, key, and value representations, three linear layers are applied to obtain X_q, X_k, and X_v, respectively:

$$X_q = [V, T]W_Q, X_k = [V, T]W_K, X_v = [V, T]W_V \tag{1}$$

Then, the attention operation is executed as:

$$\text{Attention}(X) = \text{softmax}\left(\frac{X_q X_k^T}{\sqrt{d}}\right) X_v \in \mathbb{R}^{(v+t)\times h} \tag{2}$$

Typically, a causal attention mask is applied and queries can only attend to keys preceding them in the sequence. The outputs are multiplied by another linear layer W_O to update the hidden states through a residual connection:

$$\text{SA}(X) = \text{Attention}(X)W_O + X. \tag{3}$$

3.2 NAAVIT

As analyzed in Section 2, embedding space alignment achieves superior performance and training efficiency, making it the most popular architecture in MLLMs recently. However, this architecture is inefficient during inference, attributable to the self-attention among visual tokens. In contrast, cross-attention space alignment does not perform attention among visual tokens in the language model, leading to inference efficiency. A question arises here: **Is attention among visual tokens necessary for MLLMs?**

To answer this question, we propose NAAViT (No Attention Among Visual Tokens), which eliminates attention among visual tokens. We illustrate the architecture of NAAViT in Figure 3 (Top). Specifically, for the visual-text token sequence $X = [V, T] \in \mathbb{R}^{(v+t)\times h}$, queries X_q, keys X_k and values X_v are obtained as:

$$X_q = TW_Q, X_k = [V, T]W_K, X_v = [V, T]W_V \tag{4}$$

The attention operation is executed as Equation 2, but with NAAViT attention mask, where the queries can attend to visual tokens and text tokens preceding them.

When the number of visual and text tokens is v and t respectively, the vanilla self-attention exhibits a computational complexity of $\mathcal{O}((v+t)^2)$ for the attention operation in Equation 2. By eliminating the attention among visual tokens, NAAViT reduces the complexity to $\mathcal{O}(t(v+t))$. Furthermore, since NAAViT reduces the query length from $v+t$ to t, it also significantly reduces the computational costs associated with linear layers W_Q and W_O.

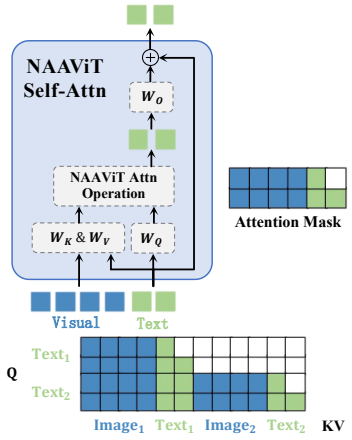

Figure 3: Top: NAAViT self-attention block. Bottom: Attention mask for interleaved image-text.

3.3 PILOT EXPERIMENT

We train a model under the same configurations as LLaVA-1.5-7B, but replace the vanilla self-attention with NAAViT.

In Table 1, we compare NAAViT and vanilla self-attention on multiple MLLM benchmarks, including MMMU Yue et al. (2024), MMBench Liu et al. (2024b), MMBench-CN Liu et al. (2024b), POPE Li et al. (2023d), ScienceQA IMG Lu et al. (2022) and OKVQA Marino et al. (2019). Among them, MMMU contains interleaved text-image inputs. For these inputs, the NAAViT attention mask is illustrated in Figure 3 (Bottom). Despite eliminating

Attention	MMMU VAL	MMBench EN	MMBench CN	POPE	ScienceQA IMG	OK-VQA
Vanilla	35.7	64.3	58.3	86.8	66.8	53.4
NAAViT	36.0	64.9	58.4	86.9	68.7	56.0

Table 1: Effects of attention mechanisms.

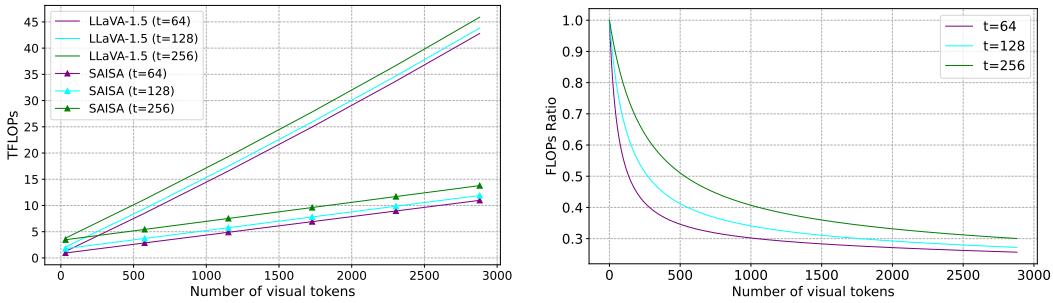

(a) TFLOPs with different numbers of tokens

(b) FLOPs ratio of SAISA and LLaVA-1.5

Figure 4: Inference computational costs comparison with different numbers of visual and text tokens, where t denotes the number of text tokens. SAISA achieves higher computational efficiency.

the attention among visual tokens, the model employing NAAViT outperforms the one using the vanilla self-attention. Given that NAAViT substantially reduces computational overhead, it offers a favorable balance between performance and efficiency.

In conclusion, attention among visual tokens is highly redundant for building MLLMs. In the following section, we introduce SAISA (Self-Attention Input Space Alignment) for efficient MLLMs based on NAAViT.

4 SAISA

4.1 Architecture

As mentioned earlier, besides the attention operation, another factor that contributes to inference inefficiency is applying FFNs to visual tokens. Based on NAAViT, which eliminates the attention among visual tokens, we propose SAISA (Self-Attention Input Space Alignment), an architecture for further enhancing MLLM efficiency. In SAISA, we also eliminate FFNs' computations on visual tokens.

We illustrate the SAISA architecture in Figure 2(c). SAISA contains a visual encoder to extract visual features, a projector, and an LLM. Each layer of the LLM consists of a self-attention block and an FFN. We utilize NAAViT in the self-attention blocks. The purpose of the projector is to directly align the visual features with the input spaces of different self-attention blocks in the LLM.

Specifically, we assume n is the number of layers in the LLM, h is the hidden size of the LLM, d is the dimension of visual features, v is the number of visual tokens, and t is the number of text tokens. For an input image I, we first employ the visual encoder VE to extract visual features:

$$Z = \text{VE}(I) \in \mathbb{R}^{v \times d} \tag{5}$$

Then, we use the projector P to directly align the visual features with the input spaces of different NAAViT self-attention blocks:

$$V = \text{P}(Z) \in \mathbb{R}^{n \times v \times h} \tag{6}$$

For the i-th NAAViT self-attention block NAAViT_i, we input the aligned visual features $V_i \in \mathbb{R}^{v \times h}$ and hidden states of the text tokens $T_i \in \mathbb{R}^{t \times h}$:

$$H_i = \text{NAAViT}_i(V_i, T_i) \in \mathbb{R}^{t \times h}, i = 1, 2, 3, \ldots, n \tag{7}$$

Notably, the NAAViT self-attention block only outputs the text tokens' hidden states H_i for the subsequent FFN, and we apply the FFN to update the text tokens:

$$T_{i+1} = \text{FFN}_i(H_i) \in \mathbb{R}^{t \times h}, i = 1, 2, 3, \ldots, n. \tag{8}$$

SAISA utilizes T_{n+1} for the next-token prediction.

Method	LLM	#Vis. Tok.	Training Data↓	Inference TFLOPs↓	MMMU VAL	MME	MMBench EN	MMBench CN	SEED-Bench
InstructBLIP	Vicuna-7B	32	130M	1.25	30.6	1137.1	36.0	23.7	58.8
MiniGPT-v2	Llama2-7B	256	326M	4.20	25.0	708.4	24.3	-	29.4
Otter	Llama-7B	64	2.1B	1.15	-	1292.3	48.3	-	35.2
Shikra	Vicuna-7B	256	6.1M	4.20	-	-	58.8	-	-
IDEFICS-9B	Llama-7B	64	354M	1.15	18.4	942.0	48.2	25.2	44.5
IDEFICS-80B	Llama-65B	64	354M	11.42	-	1244.9	54.5	38.1	53.2
Qwen-VL-Chat	Qwen-7B	256	1.4B	4.20	36.0	1435.2	60.6	56.7	65.4
FastV	Vicuna-7B	576	1.2M	4.90	35.8	-	64.3	56.8	-
VTW	Vicuna-7B	576	1.2M	4.70	36.3	-	64.0	58.5	-
MQT-LLaVA	Vicuna-7B	256	1.2M	4.20	34.8	1434.5	64.3	-	-
LLaVA-1.5	Vicuna-7B	576	1.2M	8.53	35.7	**1510.7**	64.3	58.3	**66.1**
SAISA (Ours)	Vicuna-7B	576	1.2M	2.86	**36.9**	1461.9	**65.7**	**59.0**	64.5

Table 2: Performance on comprehensive benchmarks for MLLMs. #Vis. Tok.: the number of visual tokens involved in each image. Training Data: accumulated multimodal pre-training and fine-tuning data volume. ↓: a lower value in these columns is better. Inference TFLOPs: the computational cost of processing a single image when the number of text tokens is 64. Among the baseline models, FastV, VTW and MQT-LLaVA are efficient MLLMs. The comparison between LLaVA-1.5 and SAISA is fair, because they use the same settings and training data.

4.2 Projector

Since each LLM layer operates in distinct attention spaces, the projector must flexibly align the visual features with each of the spaces. For simplicity, we employ distinct two-layer MLPs for each layer of the LLM. When the LLM has n layers, the projector contains n MLPs. Following LLaVA-1.5 Liu et al. (2024a), we set the intermediate size of each MLP to be the same as the LLM hidden size.

Specifically, for the i-th layer of the LLM,

$$V_i = \text{MLP}_i(Z) = \varphi(ZW_{i,1})W_{i,2}, i = 1, 2, 3, \ldots, n \tag{9}$$

where $Z \in \mathbb{R}^{v \times d}$ is the visual features from the visual encoder, φ is the activation function like GELU Hendrycks & Gimpel (2016), $W_{i,1} \in \mathbb{R}^{d \times h}$ and $W_{i,2} \in \mathbb{R}^{h \times h}$ are the weight matrices of the two fully connected layers.

4.3 Training Procedure

The training procedure of SAISA consists of two stages: pre-training and fine-tuning.

Pre-training. The objective of pre-training is to transform an LLM into an MLLM with a foundational comprehension of visual information, providing an initialization for the multimodal fine-tuning stage. Following LLaVA-1.5, only the multimodal projector is trainable during this stage. To improve training efficiency, we further reduce the number of trainable parameters in this stage. Specifically, we train a shared MLP for all layers of the LLM.

Fine-tuning. The objective of fine-tuning is to enable the model to follow visual instructions from users. As an initialization, we replicate the pre-trained shared MLP N times to initialize the MLPs in the projector, where N denotes the number of layers in the LLM. Following LLaVA-1.5, we utilize visual instruction data to train the model, and both the LLM and the projector are trainable during this stage.

4.4 Comparison of Computational Cost

We focus on the computations of the LLM and the projector, because those of the visual encoder are identical in this comparison. For LLM with n layers, we assume h is the hidden state size, m is the intermediate size of the FFNs, t is the number of text tokens, and v is the number of visual tokens. To comprehensively consider LLMs with and without grouped query attention (GQA) Ainslie et al. (2023), we assume that k is the output dimension of key/value matrices. For the projector, we

Method	LLM	Inference TFLOPs↓	POPE overall	POPE rand	POPE pop	POPE adv	GQA	ScienceQA IMG	TextVQA	OK-VQA
Shikra	Vicuna-7B	4.20	84.7	86.9	84.0	83.1	-	-	-	-
IDEFICS	Llama-7B	1.67	81.8	88.3	81.1	76.0	35.5	51.6	25.9	38.4
IDEFICS	Llama-65B	16.62	77.5	86.7	74.9	70.8	45.2	61.8	30.9	45.2
Qwen-VL-Chat	Qwen-7B	4.20	87.0	**89.0**	87.4	84.7	57.5	68.2	**61.5**	56.6
LLaVA-1.5	Vicuna-7B	8.53	86.8	88.2	87.2	**85.1**	**62.0**	66.8	58.2	53.4
SAISA (Ours)	Vicuna-7B	2.86	**87.2**	**89.0**	**87.6**	85.0	60.9	**70.1**	56.8	**56.8**

Table 3: Performance on hallucination and VQA benchmarks. The comparison between LLaVA-1.5 and SAISA is fair.

assume that d is the dimension of the input visual features. The FLOPs of LLaVA-1.5 are $2n(t+v)h(2h+3m+2k)+4n(t+v)^2h+2vhd+2vh^2$ For SAISA, visual tokens are multiplied only by the key and value matrices, and the query sequence length is t in the attention operation. Therefore, the FLOPs are $2nth(2h+3m+2k)+4nvhk+4nt(t+v)h+2nvhd+2nvh^2$. Details of the FLOPs calculation are in the Supplementary Material. Figure 4 compares the FLOPs of SAISA and LLaVA-1.5 with different numbers of tokens, based on Vicuna-7B-v1.5 Chiang et al. (2023). We can observe that SAISA achieves a higher computational efficiency than LLAVA-1.5 when processing the same numbers of tokens.

5 Experiments

5.1 Setups

Model Configuration. We mainly compare SAISA with LLaVA-1.5 Liu et al. (2024a) due to its fully open training data, replicability, and acceptable training costs. We use the same settings as LLaVA-1.5. To be specific, we employ Vicuna-7B-v1.5 Chiang et al. (2023) as the default LLM backbone and CLIP-ViT-L/14-336 Radford et al. (2021) as the default visual encoder.

Training Details. We utilize the same training data as LLaVA-1.5. The pre-training dataset contains 558k samples, and the fine-tuning dataset contains 665k samples.

5.2 Main Results

The performance on benchmarks is shown in Table 2 and 3. The inference latency test is shown in Table 4. We also include efficient MLLMs in both training-based and training-free manners, such as MQT-LLaVA Hu et al. (2024), FastV Chen et al. (2024) and VTW Lin et al. (2024).

Method	64 Text Tok. Latency (ms)	128 Text Tok. Latency (ms)	256 Text Tok. Latency (ms)
LLaVA-1.5	56.0	64.4	75.6
SAISA (Ours)	33.0	37.1	45.9

Table 4: Results of the inference latency test.

We evaluate SAISA on a range of benchmarks, including: (1) comprehensive benchmarks for instruction-following MLLMs such as MMMU Yue et al. (2024), MME Fu et al. (2023), MM-Bench Liu et al. (2024b), MMBench-CN Liu et al. (2024b), and SEED-Bench Li et al. (2023b); (2) hallucination benchmark such as POPE Li et al. (2023d), which evaluates MLLMs' degree of hallucination on three subsets: random, popular, and adversarial; (3) general visual question answering benchmarks such as GQA Hudson & Manning (2019) and ScienceQA IMG Lu et al. (2022); (4) fine-grained visual question answering benchmarks such as OK-VQA Marino et al. (2019) and TextVQA Singh et al. (2019), OK-VQA requires fine-grained image understanding and spatial understanding, and TextVQA is an OCR-related benchmark; (5) vision-centric MLLM benchmarks such as MMVP Tong et al. (2024) and CV-Bench Tong et al. (2025). We report the TFLOPs of processing a single image when the number of text tokens is 64. In the inference latency test, the latency is reported as the time of LLM prefilling during inference with varying numbers of text tokens.

Table 2 shows the comparison on the comprehensive benchmarks. rictSAISA outperforms InstructBLIP Dai et al. (2023), MiniGPT-v2Chen et al. (2023a), Otter Li et al. (2023a), Shikra Chen et al.

Method	LLM	Visual Encoder	#Vis. Tok.	Inference TFLOPs↓	MMMU VAL	MMBench EN	MMBench CN	POPE	GQA	SQA IMG	OK-VQA	Average
LLaVA-1.5	Vicuna	SigLIP	729	10.63	36.6	66.2	58.9	86.5	62.5	**70.5**	**56.4**	62.5
SAISA (Ours)	Vicuna	SigLIP	729	3.40	**37.4**	**67.5**	**60.7**	**87.0**	**62.9**	70.0	55.8	**63.0**
LLaVA-1.5	Vicuna	Conv	1024	14.76	34.6	56.6	49.6	**88.2**	**61.1**	66.4	51.4	58.3
SAISA (Ours)	Vicuna	Conv	1024	4.44	**35.1**	**61.1**	**54.9**	87.0	57.7	**66.5**	**54.4**	**59.5**
LLaVA-1.5	Vicuna	CLIP	576	8.53	35.7	64.3	58.3	86.8	**62.0**	66.8	53.4	61.0
SAISA (Ours)	Vicuna	CLIP	576	2.86	**36.9**	**65.7**	**59.0**	**87.2**	60.9	**70.1**	**56.8**	**62.4**
LLaVA-1.5	Mistral	CLIP	576	9.17	34.8	65.9	54.9	**87.2**	**62.0**	**71.6**	2.5*	54.1
SAISA (Ours)	Mistral	CLIP	576	2.10	**35.9**	**67.5**	**57.5**	86.9	61.2	71.2	**23.9***	**57.7**
LLaVA-1.5	Llama3	CLIP	576	9.17	36.8	70.4	64.2	**87.2**	**63.5**	73.3	**61.2**	65.2
SAISA (Ours)	Llama3	CLIP	576	2.10	**38.3**	**71.3**	**65.2**	86.8	61.8	**74.4**	60.7	**65.6**

Table 5: Ablation on LLMs and Visual Encoders. Here, "SigLIP" = SigLIP-ViT-SO400M/14-384, "Conv" = OpenCLIP-ConvNeXt-XXL-1024, and "CLIP" = CLIP-ViT-L/14-336. *Both LLaVA-1.5 and SAISA models on Mistral exhibit low performance on OK-VQA, because they respond to most questions in this benchmark with "Unanswerable".

Pre-trained Parameters	MMMU VAL	MMBench EN	MMBench CN	POPE	SQA IMG	OK-VQA
Full Projector	34.8	59.2	51.1	85.6	67.8	53.1
Shared MLP	36.9	65.7	59.0	87.2	70.1	56.8

Table 6: Ablation on Pre-training Strategies.

Projector	MMMU VAL	MMBench EN	MMBench CN	POPE	SQA IMG	OK-VQA
Linear Layers	35.7	65.3	56.6	85.8	69.2	53.6
Resamplers	35.6	59.5	50.5	83.5	69.1	53.4
MLPs	36.9	65.7	59.0	87.2	70.1	56.8

Table 7: Ablation on Projector Designs.

(2023b), and IDEFICS IDEFICS (2023) utilizing LLama-7B and LLama-65B Touvron et al. (2023a) across all these benchmarks. Compared with Qwen-VL-Chat Bai et al. (2023b) and LLaVA-1.5 Liu et al. (2024a), SAISA performs better on most benchmarks. Among these baseline models, Otter and IDEFICS employ cross-attention space alignment, whereas the other models utilize embedding space alignment. Table 3 shows the comparison on the hallucination and VQA benchmarks. We also include the comparison on vision-centric benchmarks in the appendix. SAISA achieves the best overall performance compared to the baseline, and strikes a favorable balance between performance and efficiency.

Notably, SAISA inherently supports flexible multi-turn conversations. We include multi-turn results in the appendix.

5.3 Ablation Study

Ablation on LLMs and Visual Encoders. As presented in Table 5, we perform multiple ablation experiments on both LLM backbones and visual encoders to validate the effectiveness of SAISA. We tune a set of SAISA models using a variety of LLM backbones and visual encoders. The ablated LLMs include Vicuna-7B Chiang et al. (2023) and two LLMs using grouped query attention (GQA) Ainslie et al. (2023), such as Mistral-7B Jiang et al. (2023) and Llama3-8B Meta (2024). The ablated visual encoders include two ViT-based Dosovitskiy et al. (2020) visual backbones such as CLIP-ViT-L/14-336 Radford et al. (2021) and SigLIP-ViT-SO400M/14-384 Zhai et al. (2023), and a ConvNeXt-based Liu et al. (2022) visual encoder such as ConvNeXt-XXL-1024 from OpenCLIP Ilharco et al. (2021); Schuhmann et al. (2022). The experimental results demonstrate that SAISA consistently achieves superior performance to LLaVA-1.5 across different LLM backbones and visual encoders, while dramatically reducing computational costs.

Ablation on Pre-training Strategies. As shown in Table 6, we conduct an ablation to investigate the effects of SAISA's pre-training strategies. We tune a SAISA model where the full projector (32 MLPs) is tunable during pre-training, and the other settings keep the same as the original SAISA. With more randomly initialized parameters, we observe a performance drop when pre-training the full projector. We attribute this drop to the small amount of pre-training data with only 558k samples. This ablation study demonstrates the effectiveness of our pre-training strategy, which provides a robust initialization for the subsequent fine-tuning stage.

Ablation on Projector Designs. Previous studies find that replacing linear projection with MLP projection improves performance in MLLM Liu et al. (2024a) and self-supervised learning Chen et al. (2020a;b). We conduct an experiment to investigate the impact of projector designs in SAISA. We tune a model under the same configuration as the original SAISA model but replace each MLP in the projector with a linear layer or a resampler Jaegle et al. (2021). We set the output token number of the resampler projector to 256. Table 7 shows that the model with the MLP projector performs better than the model with other projectors, including the linear projector, which is consistent with the finding of the previous study Liu et al. (2024a). Furthermore, the linear projector performs better than the resampler projector, because the latter down-samples visual tokens and overlooks fine-grained visual information such as spatial information.

6 Related Work

6.1 Multimodal Large Language Models

Multimodal Large Language Models (MLLMs) are typically built on Large Language Models (LLMs) Chiang et al. (2023); Meta (2024); Jiang et al. (2023); Touvron et al. (2023a;b); Bai et al. (2023a) by aligning visual features generated by visual encoders Radford et al. (2021); Zhai et al. (2023); Ilharco et al. (2021); Liu et al. (2022) with the LLMs. There are two most common architectures for this purpose, embedding space alignment and cross-attention space alignment. For embedding space alignment Liu et al. (2023; 2024a); Li et al. (2023c); Dai et al. (2023); Bai et al. (2023b); Chen et al. (2023a); Zhu et al. (2023); Bai et al. (2025); Zhu et al. (2025), MLLMs align visual features with the text token embedding space via a projector and concatenate the visual and text tokens as the LLM input. These models exhibit efficiency during training, but suffer from inference inefficiency because of the long token sequence. For cross-attention space alignment Alayrac et al. (2022); LAION (2023); Awadalla et al. (2023), MLLMs introduce new cross-attention blocks for the interaction between text and visual modalities, and align the visual features with the cross-attention spaces. These models achieve efficiency during inference, but require a substantial amount of data to train the new parameters. In this paper, we propose SAISA, an architecture for building MLLMs with efficiency during both training and inference.

6.2 Efficiency Optimization for MLLMs

To reduce the computational costs of MLLMs, previous work mainly falls into two categories: model architecture and token reduction. For model architecture, Qwen-VL Bai et al. (2023b) and BLIP series Li et al. (2023c); Dai et al. (2023) utilize attention-based mechanisms to down-sample visual tokens before they are fed into LLMs. Ye *et al.* Ye et al. (2024) incorporate cross-attention operation in parallel with self-attention, and utilizes adaptive gates for hidden states fusing. Ma *et al.* Ma et al. (2024) introduce aligners to update visual tokens in the MLLM, but the aligners still involve substantial computational overhead. For token reduction, token pruning methods Shang et al. (2024); Wang et al. (2024), *e.g.* FastV Chen et al. (2024), focus on certain "anchor" tokens and prune the other visual tokens. VTW Lin et al. (2024) removes visual tokens after a certain layer. In this paper, we investigate redundancy within the MLLM architecture and propose SAISA. Instead of directly reducing visual token number, SAISA achieves efficiency while maintaining fine-grained visual understanding by preserving the original number of visual tokens.

7 Conclusion

In this paper, we take a step towards developing MLLMs with efficiency during both training and inference. To achieve this, we conduct a study of current MLLM architectures and find the key factors for building efficient MLLMs. By integrating these factors and gradually reducing redundant computations, we propose **SAISA**, an effective and efficient architecture for MLLMs. SAISA demonstrates the ability to dramatically reduce the computational costs of MLLMs without compromising their capabilities.

REFERENCES

Josh Achiam, Steven Adler, Sandhini Agarwal, Lama Ahmad, Ilge Akkaya, Florencia Leoni Aleman, Diogo Almeida, Janko Altenschmidt, Sam Altman, Shyamal Anadkat, et al. Gpt-4 technical report. *arXiv preprint arXiv:2303.08774*, 2023.

Joshua Ainslie, James Lee-Thorp, Michiel De Jong, Yury Zemlyanskiy, Federico Lebrón, and Sumit Sanghai. Gqa: Training generalized multi-query transformer models from multi-head checkpoints. *arXiv preprint arXiv:2305.13245*, 2023.

Jean-Baptiste Alayrac, Jeff Donahue, Pauline Luc, Antoine Miech, Iain Barr, Yana Hasson, Karel Lenc, Arthur Mensch, Katherine Millican, Malcolm Reynolds, et al. Flamingo: a visual language model for few-shot learning. *Advances in neural information processing systems*, 35:23716–23736, 2022.

Anas Awadalla, Irena Gao, Josh Gardner, Jack Hessel, Yusuf Hanafy, Wanrong Zhu, Kalyani Marathe, Yonatan Bitton, Samir Gadre, Shiori Sagawa, et al. Openflamingo: An open-source framework for training large autoregressive vision-language models. *arXiv preprint arXiv:2308.01390*, 2023.

Jinze Bai, Shuai Bai, Yunfei Chu, Zeyu Cui, Kai Dang, Xiaodong Deng, Yang Fan, Wenbin Ge, Yu Han, Fei Huang, et al. Qwen technical report. *arXiv preprint arXiv:2309.16609*, 2023a.

Jinze Bai, Shuai Bai, Shusheng Yang, Shijie Wang, Sinan Tan, Peng Wang, Junyang Lin, Chang Zhou, and Jingren Zhou. Qwen-vl: A versatile vision-language model for understanding, localization, text reading, and beyond. *arXiv preprint arXiv:2308.12966*, 2023b.

Shuai Bai, Keqin Chen, Xuejing Liu, Jialin Wang, Wenbin Ge, Sibo Song, Kai Dang, Peng Wang, Shijie Wang, Jun Tang, et al. Qwen2. 5-vl technical report. *arXiv preprint arXiv:2502.13923*, 2025.

Jun Chen, Deyao Zhu, Xiaoqian Shen, Xiang Li, Zechun Liu, Pengchuan Zhang, Raghuraman Krishnamoorthi, Vikas Chandra, Yunyang Xiong, and Mohamed Elhoseiny. Minigpt-v2: large language model as a unified interface for vision-language multi-task learning. *arXiv preprint arXiv:2310.09478*, 2023a.

Keqin Chen, Zhao Zhang, Weili Zeng, Richong Zhang, Feng Zhu, and Rui Zhao. Shikra: Unleashing multimodal llm's referential dialogue magic. *arXiv preprint arXiv:2306.15195*, 2023b.

Liang Chen, Haozhe Zhao, Tianyu Liu, Shuai Bai, Junyang Lin, Chang Zhou, and Baobao Chang. An image is worth 1/2 tokens after layer 2: Plug-and-play inference acceleration for large vision-language models. In *European Conference on Computer Vision*, pp. 19–35. Springer, 2024.

Ting Chen, Simon Kornblith, Mohammad Norouzi, and Geoffrey Hinton. A simple framework for contrastive learning of visual representations. In *International conference on machine learning*, pp. 1597–1607. PmLR, 2020a.

Xinlei Chen, Haoqi Fan, Ross Girshick, and Kaiming He. Improved baselines with momentum contrastive learning. *arXiv preprint arXiv:2003.04297*, 2020b.

Wei-Lin Chiang, Zhuohan Li, Zi Lin, Ying Sheng, Zhanghao Wu, Hao Zhang, Lianmin Zheng, Siyuan Zhuang, Yonghao Zhuang, Joseph E. Gonzalez, Ion Stoica, and Eric P. Xing. Vicuna: An open-source chatbot impressing gpt-4 with 90%* chatgpt quality, March 2023. URL https://lmsys.org/blog/2023-03-30-vicuna/.

Wenliang Dai, Junnan Li, DONGXU LI, Anthony Tiong, Junqi Zhao, Weisheng Wang, Boyang Li, Pascale N Fung, and Steven Hoi. Instructblip: Towards general-purpose vision-language models with instruction tuning. In A. Oh, T. Naumann, A. Globerson, K. Saenko, M. Hardt, and S. Levine (eds.), *Advances in Neural Information Processing Systems*, volume 36, pp. 49250–49267. Curran Associates, Inc., 2023. URL https://proceedings.neurips.cc/paper_files/paper/2023/file/9a6a435e75419a836fe47ab6793623e6-Paper-Conference.pdf.

Wenliang Dai, Nayeon Lee, Boxin Wang, Zhuolin Yang, Zihan Liu, Jon Barker, Tuomas Rintamaki, Mohammad Shoeybi, Bryan Catanzaro, and Wei Ping. Nvlm: Open frontier-class multimodal llms. *arXiv preprint arXiv:2409.11402*, 2024.

Alexey Dosovitskiy, Lucas Beyer, Alexander Kolesnikov, Dirk Weissenborn, Xiaohua Zhai, Thomas Unterthiner, Mostafa Dehghani, Matthias Minderer, Georg Heigold, Sylvain Gelly, et al. An image is worth 16x16 words: Transformers for image recognition at scale. *arXiv preprint arXiv:2010.11929*, 2020.

Chaoyou Fu, Peixian Chen, Yunhang Shen, Yulei Qin, Mengdan Zhang, Xu Lin, Jinrui Yang, Xiawu Zheng, Ke Li, Xing Sun, et al. Mme: A comprehensive evaluation benchmark for multimodal large language models. *arXiv preprint arXiv:2306.13394*, 2023.

Dan Hendrycks and Kevin Gimpel. Gaussian error linear units (gelus). *arXiv preprint arXiv:1606.08415*, 2016.

Wenbo Hu, Zi-Yi Dou, Liunian Harold Li, Amita Kamath, Nanyun Peng, and Kai-Wei Chang. Matryoshka query transformer for large vision-language models. *arXiv preprint arXiv:2405.19315*, 2024.

Drew A Hudson and Christopher D Manning. Gqa: A new dataset for real-world visual reasoning and compositional question answering. In *Proceedings of the IEEE/CVF conference on computer vision and pattern recognition*, pp. 6700–6709, 2019.

IDEFICS. Introducing idefics: An open reproduction of state-of-the-art visual language model. `https://huggingface.co/blog/idefics`, 2023.

Gabriel Ilharco, Mitchell Wortsman, Ross Wightman, Cade Gordon, Nicholas Carlini, Rohan Taori, Achal Dave, Vaishaal Shankar, Hongseok Namkoong, John Miller, Hannaneh Hajishirzi, Ali Farhadi, and Ludwig Schmidt. Openclip, jul 2021. URL `https://doi.org/10.5281/zenodo.5143773`.

Andrew Jaegle, Felix Gimeno, Andy Brock, Oriol Vinyals, Andrew Zisserman, and Joao Carreira. Perceiver: General perception with iterative attention. In *International conference on machine learning*, pp. 4651–4664. PMLR, 2021.

Albert Q. Jiang, Alexandre Sablayrolles, Arthur Mensch, Chris Bamford, Devendra Singh Chaplot, Diego de las Casas, Florian Bressand, Gianna Lengyel, Guillaume Lample, Lucile Saulnier, Lélio Renard Lavaud, Marie-Anne Lachaux, Pierre Stock, Teven Le Scao, Thibaut Lavril, Thomas Wang, Timothée Lacroix, and William El Sayed. Mistral 7b. *arXiv preprint arXiv:2310.06825*, 2023.

LAION. Openflamingo v2: New models and enhanced training setup. `https://laion.ai/blog/open-flamingo-v2/`, 2023. Accessed: 2024-05-26.

Bo Li, Yuanhan Zhang, Liangyu Chen, Jinghao Wang, Jingkang Yang, and Ziwei Liu. Otter: A multi-modal model with in-context instruction tuning. *arXiv preprint arXiv:2305.03726*, 2023a.

Bohao Li, Rui Wang, Guangzhi Wang, Yuying Ge, Yixiao Ge, and Ying Shan. Seed-bench: Benchmarking multimodal llms with generative comprehension. *arXiv preprint arXiv:2307.16125*, 2023b.

Junnan Li, Dongxu Li, Silvio Savarese, and Steven Hoi. Blip-2: Bootstrapping language-image pre-training with frozen image encoders and large language models. In *International conference on machine learning*, pp. 19730–19742. PMLR, 2023c.

Yifan Li, Yifan Du, Kun Zhou, Jinpeng Wang, Wayne Xin Zhao, and Ji-Rong Wen. Evaluating object hallucination in large vision-language models. *arXiv preprint arXiv:2305.10355*, 2023d.

Zhihang Lin, Mingbao Lin, Luxi Lin, and Rongrong Ji. Boosting multimodal large language models with visual tokens withdrawal for rapid inference. *arXiv preprint arXiv:2405.05803*, 2024.

Ziyi Lin, Chris Liu, Renrui Zhang, Peng Gao, Longtian Qiu, Han Xiao, Han Qiu, Chen Lin, Wenqi Shao, Keqin Chen, et al. Sphinx: The joint mixing of weights, tasks, and visual embeddings for multi-modal large language models. *arXiv preprint arXiv:2311.07575*, 2023.

Haotian Liu, Chunyuan Li, Qingyang Wu, and Yong Jae Lee. Visual instruction tuning. *Advances in neural information processing systems*, 36:34892–34916, 2023.

Haotian Liu, Chunyuan Li, Yuheng Li, and Yong Jae Lee. Improved baselines with visual instruction tuning. In *Proceedings of the IEEE/CVF Conference on Computer Vision and Pattern Recognition*, pp. 26296–26306, 2024a.

Yuan Liu, Haodong Duan, Yuanhan Zhang, Bo Li, Songyang Zhang, Wangbo Zhao, Yike Yuan, Jiaqi Wang, Conghui He, Ziwei Liu, et al. Mmbench: Is your multi-modal model an all-around player? In *European conference on computer vision*, pp. 216–233. Springer, 2024b.

Zhuang Liu, Hanzi Mao, Chao-Yuan Wu, Christoph Feichtenhofer, Trevor Darrell, and Saining Xie. A convnet for the 2020s. In *Proceedings of the IEEE/CVF conference on computer vision and pattern recognition*, pp. 11976–11986, 2022.

Pan Lu, Swaroop Mishra, Tanglin Xia, Liang Qiu, Kai-Wei Chang, Song-Chun Zhu, Oyvind Tafjord, Peter Clark, and Ashwin Kalyan. Learn to explain: Multimodal reasoning via thought chains for science question answering. *Advances in Neural Information Processing Systems*, 35:2507–2521, 2022.

Feipeng Ma, Yizhou Zhou, Hebei Li, Zilong He, Siying Wu, Fengyun Rao, Yueyi Zhang, and Xiaoyan Sun. Ee-mllm: A data-efficient and compute-efficient multimodal large language model. *arXiv preprint arXiv:2408.11795*, 2024.

Kenneth Marino, Mohammad Rastegari, Ali Farhadi, and Roozbeh Mottaghi. Ok-vqa: A visual question answering benchmark requiring external knowledge. In *Proceedings of the IEEE/cvf conference on computer vision and pattern recognition*, pp. 3195–3204, 2019.

Meta. Introducing meta llama 3: The most capable openly available llm to date. `https://ai.meta.com/blog/meta-llama-3/`, 2024. Accessed: 2024-05-26.

OpenAI. Gpt-4v(ision) system card. `https://cdn.openai.com/papers/GPTV_System_Card.pdf`, 2023.

Alec Radford, Jong Wook Kim, Chris Hallacy, Aditya Ramesh, Gabriel Goh, Sandhini Agarwal, Girish Sastry, Amanda Askell, Pamela Mishkin, Jack Clark, et al. Learning transferable visual models from natural language supervision. In *International conference on machine learning*, pp. 8748–8763. PmLR, 2021.

Christoph Schuhmann, Romain Beaumont, Richard Vencu, Cade Gordon, Ross Wightman, Mehdi Cherti, Theo Coombes, Aarush Katta, Clayton Mullis, Mitchell Wortsman, et al. Laion-5b: An open large-scale dataset for training next generation image-text models. *Advances in neural information processing systems*, 35:25278–25294, 2022.

Yuzhang Shang, Mu Cai, Bingxin Xu, Yong Jae Lee, and Yan Yan. Llava-prumerge: Adaptive token reduction for efficient large multimodal models. *arXiv preprint arXiv:2403.15388*, 2024.

Amanpreet Singh, Vivek Natarajan, Meet Shah, Yu Jiang, Xinlei Chen, Dhruv Batra, Devi Parikh, and Marcus Rohrbach. Towards vqa models that can read. In *Proceedings of the IEEE/CVF conference on computer vision and pattern recognition*, pp. 8317–8326, 2019.

Peter Tong, Ellis Brown, Penghao Wu, Sanghyun Woo, Adithya Jairam Vedagiri IYER, Sai Charitha Akula, Shusheng Yang, Jihan Yang, Manoj Middepogu, Ziteng Wang, et al. Cambrian-1: A fully open, vision-centric exploration of multimodal llms. *Advances in Neural Information Processing Systems*, 37:87310–87356, 2025.

Shengbang Tong, Zhuang Liu, Yuexiang Zhai, Yi Ma, Yann LeCun, and Saining Xie. Eyes wide shut? exploring the visual shortcomings of multimodal llms. In *Proceedings of the IEEE/CVF Conference on Computer Vision and Pattern Recognition*, pp. 9568–9578, 2024.

Hugo Touvron, Thibaut Lavril, Gautier Izacard, Xavier Martinet, Marie-Anne Lachaux, Timothée Lacroix, Baptiste Rozière, Naman Goyal, Eric Hambro, Faisal Azhar, et al. Llama: Open and efficient foundation language models. *arXiv preprint arXiv:2302.13971*, 2023a.

Hugo Touvron, Louis Martin, Kevin Stone, Peter Albert, Amjad Almahairi, Yasmine Babaei, Nikolay Bashlykov, Soumya Batra, Prajjwal Bhargava, Shruti Bhosale, et al. Llama 2: Open foundation and fine-tuned chat models. *arXiv preprint arXiv:2307.09288*, 2023b.

Ao Wang, Fengyuan Sun, Hui Chen, Zijia Lin, Jungong Han, and Guiguang Ding. [cls] token tells everything needed for training-free efficient mllms. *arXiv preprint arXiv:2412.05819*, 2024.

Jiabo Ye, Haiyang Xu, Haowei Liu, Anwen Hu, Ming Yan, Qi Qian, Ji Zhang, Fei Huang, and Jingren Zhou. mplug-owl3: Towards long image-sequence understanding in multi-modal large language models. In *The Thirteenth International Conference on Learning Representations*, 2024.

Xiang Yue, Yuansheng Ni, Kai Zhang, Tianyu Zheng, Ruoqi Liu, Ge Zhang, Samuel Stevens, Dongfu Jiang, Weiming Ren, Yuxuan Sun, et al. Mmmu: A massive multi-discipline multimodal understanding and reasoning benchmark for expert agi. In *Proceedings of the IEEE/CVF Conference on Computer Vision and Pattern Recognition*, pp. 9556–9567, 2024.

Xiaohua Zhai, Basil Mustafa, Alexander Kolesnikov, and Lucas Beyer. Sigmoid loss for language image pre-training. In *Proceedings of the IEEE/CVF international conference on computer vision*, pp. 11975–11986, 2023.

Deyao Zhu, Jun Chen, Xiaoqian Shen, Xiang Li, and Mohamed Elhoseiny. Minigpt-4: Enhancing vision-language understanding with advanced large language models. *arXiv preprint arXiv:2304.10592*, 2023.

Jinguo Zhu, Weiyun Wang, Zhe Chen, Zhaoyang Liu, Shenglong Ye, Lixin Gu, Hao Tian, Yuchen Duan, Weijie Su, Jie Shao, et al. Internvl3: Exploring advanced training and test-time recipes for open-source multimodal models. *arXiv preprint arXiv:2504.10479*, 2025.

A APPENDIX

A.1 LLM USAGE

We used OpenAI's ChatGPT to help polish the language and improve the readability of the manuscript. Specifically, ChatGPT was used for grammar checking and sentence rephrasing. We list our prompt for using OpenAI's ChatGPT to help polish writing as follows.

Prompt for Using OpenAI's ChatGPT to Help Polish Writing

```
Below is a paragraph from an academic paper. Polish the
   writing to meet the academic style,improve the spelling,
   grammar, clarity, concision and overall readability.
   Furthermore, list all modification and explain the
   reasons to do so in markdown table. \\
Paragraph: {paragraph}
```

A.2 ANALYSIS OF COMPUTATIONAL OVERHEAD

In this section, we provide details of the calculation of the FLOPs of SAISA and LLaVA-1.5. compare the computational costs of SAISA and LLaVA-1.5. We consider the computations of the LLM and the projector, as the computations of the visual encoder are identical in comparison. We consider the computations of the self-attention blocks and the FFNs in each layer of the LLM.

We denote the hidden state size of the LLM backbone as h, and the output dimension of the W_K, W_V matrices is k. When the token sequence has l tokens, the FLOPs of a vanilla self-attention block contain those of the W_Q, W_K, W_V and W_O matrices, as well as the self-attention operation. The FLOPs of each of W_K, W_V are $2lhk$, and those of each of W_Q and W_O are $2lh^2$, and the FLOPs of the self-attention operation are $4l^2h$. The overall FLOPs of the vanilla self-attention block are $4lh^2 + 4lhk + 4l^2h$. For an feed-forward network (FFN), we assume that their intermediate size is m, and the FLOPs are $6lhm$. When the LLM backbone has n layers, the FLOPs are $2nlh(2h + 3m + 2k) + 4nl^2h$.

We use v to denote the number of visual tokens, and t to denote the number of text tokens. For LLaVA-1.5, the visual and text tokens are concatenated and then fed into the LLM backbone, resulting in $v + t$ tokens. As a result, the FLOPs of the LLM backbone are $2n(v + t)h(2h + 3m + 2k) + 4(v + t)l^2h$. For the 2-layer MLP projector, where the hidden layer size is set to h, the FLOPs of the first layer are $2vhd$, and those of the second layer are $2vh^2$. The overall FLOPs of LLaVA-1.5 are $2n(v + t)h(2h + 3m + 2k) + 4(v + t)l^2h$.

For SAISA, a NAAViT self-attention block also contains W_Q, W_K, W_V, W_O and the self-attention operation. In contrast to the vanilla self-attention block, the W_Q and W_O matrices are only applied to text tokens in SAISA, and the attention operation among visual tokens are omitted. As a result, the overall FLOPs of a NAAViT self-attention block are $2th(2h + 2k) + 4vhk + 4t(t + v)h$. The FFNs in SAISA are only applied to text tokens, resulting in FLOPs $6thm$. With respect to the projector, which contains n 2-layer MLPs, the FLOPs are $2nvhd + 2nvh^2$. The overall FLOPs of SAISA are $2nth(2h + 3m + 2k) + 4nvhk + 4nt(t + v)h + 2nvhd + 2nvh^2$.

A.3 IMPLEMENT DETAILS

The detailed training settings and hyperparameters (HPs) of SAISA are summarized in Table 8, including the hyperparameters utilized during the pre-training and fine-tuning. The entire two-stage training process of SAISA is executed on a single node with 8 NVIDIA A800 80G GPUs, employing flash-attention v2 for all experiments.

Configurations	Pre-training	Fine-tuning
Projector Init.	Random	Pre-training Stage
Training Modules	Shared MLP	Projector, LLM
Deepspeed	zero-2	zero-3
Learning Rate	1e-3	2e-5
Warm-up Ratio	0.03	
Batch Size	256	128
Bfloat16	True	
LR Schedule	Cosine Decay	
Training Steps	2.2k	5.2k
Weight Decay	0.0	
Epoch	1	
Optimizer	AdamW	

Table 8: Hyperparameters utilized during training. LR schedule denotes learning rate schedule. Init. denotes initialization.

Method	Inference TFLOPs↓	MMVP	CV-Bench 2D	CV-Bench 3D
LLaVA-1.5	8.53	24.7	**56.6**	59.5
SAISA (Ours)	2.86	**26.0**	56.2	**59.8**

Table 9: Performance on vision-centric benchmarks.

A.4 Vision-Centric Benchmarks

In this section, we provide the comparison on vision-centric benchmarks. Since most previous methods do not evaluate their performance on these benchmarks, we compare SAISA with LLaVA-1.5. The results are shown in Table 9.

A.5 Qualitative Results

In this section, we utilize the qualitative examples in the original LLaVA-1.5 paper to comprehensively demonstrate the abilities of SAISA. The examples, which cover a diverse range of scenarios and challenges, are shown in Table 12, 11, 13 and 14. For comparison, we prompt queries in these examples to LLaVA-1.5 and include its response in most examples. Our SAISA, trained on the same data as LLaVA-1.5, demonstrates similar performance across various unseen response format prompts, while exhibiting superior training and inference efficiency. It can support flexible multi-turn conversations (Table 10) and accurately identify factual inaccuracies in questions and provide more effective and reasonable responses to complex queries (Table 12). SAISA also generates fine-grained prompts for Stable Diffusion models in a specified format (Table 11). Furthermore, it can offer responses with adjustable levels of detail based on user needs, adapting its output across multiple dialogue rounds (Table 13), and it can perform detailed writing tasks based on the given image (Table 14).

Multi-turn Conversation:	
	
User	What is unusual about this image? **Answer briefly with a single sentence.**
LLaVA-1.5	A man is hanging clothes on a clothesline attached to a car.
SAISA	A man is ironing clothes while standing on the back of a taxi.
User	**Give a more detailed explanation.**
LLaVA-1.5	A man is hanging clothes on a clothesline attached to a car, which is an unusual sight as people typically hang clothes on a clothesline at home or in a designated area.
SAISA	The unusual aspect of this image is that a man is ironing clothes while standing on the back of a taxi. This is not a typical scene, as ironing clothes is usually done indoors, and standing on the back of a moving vehicle is not a safe or practical way to do it. The man's actions may be a stunt or a publicity stunt, but it is certainly an unconventional and potentially dangerous situation.

Table 10: SAISA can dynamically adjust response granularity across multiple dialogue rounds.

Visual input example, Constrained SD Prompt Generation:	
	
User	Here's a formula for a Stable Diffusion image prompt: a cartoon-style image of [adjective] [subject] [haircut] [clothing] [doing action], [color scheme], detailed, trending on artstation. Generate the prompt for this image.
LLaVA-1.5	A cartoon-style image of a young girl with a heart-shaped bow in her hair, wearing a white and pink jacket, and holding a stuffed bunny. The image has a watercolor color scheme, and it is detailed and trending on ArtStation.
SAISA	A cartoon-style image of a young girl with a cute haircut, wearing a white jacket and a bow, holding a stuffed animal and a backpack. The image has a color scheme of pink, white, and orange, and is detailed and trending on ArtStation.

Table 11: SAISA can generating prompts in a specified format tailored for Stable Diffusion models.

Visual input example, Tricky Question:	
	
User	If there are factual errors in the questions, point it out; if not, proceed to answering the question. What's happening in the desert?
LLaVA-1.5	There is no desert in the image. The image features a beach with a city skyline in the background, and a large body of water.
SAISA	In the image, there is no desert visible. The scene takes place on a beach with a city skyline in the background. The beach is located near a city, and there is a lively atmosphere with lights reflecting on the water.

Table 12: SAISA can evaluate whether the question contains factual inaccuracies and respond to challenging questions.

Visual input example, Different Format Prompts:	
	
User	What is the color of the shirt that the man is wearing? **Answer the question using a single word or phrase.**
LLaVA-1.5	Yellow
SAISA	Yellow
User	Is this unusual? **Please explain briefly with a short sentence.**
LLaVA-1.5	Yes, it is unusual for a man to be drying clothes on the back of a moving vehicle.
SAISA	Yes, it is unusual for a man to be ironing clothes while standing on the back of a taxi.
User	Is this unusual? **Please explain in detail.**
LLaVA-1.5	Yes, this is an unusual scene. In the image, a man is sitting on a folding chair in the back of a yellow taxi, holding a clothesline with clothes on it. This is not a typical sight in a city setting, as people usually do not transport laundry in such a manner. It is also uncommon to see someone sitting on a folding chair in the back of a taxi, as passengers usually sit inside the vehicle. The combination of the man's unusual activity and the unconventional seating arrangement makes this scene stand out as an atypical and intriguing moment.
SAISA	Yes, this is an unusual scene. In the image, a man is standing on the back of a yellow taxi, holding a clothes iron. This is not a typical sight, as people usually do not use taxis for ironing clothes. It is also not common to see someone ironing clothes in public, as it is generally done indoors in a private setting, such as a home or an office. The man's actions in the image are unconventional and seem to be a humorous or artistic representation of an everyday situation.

Table 13: SAISA is capable of providing responses at various levels of granularity according to user requirements.

Visual input example, Visual Writing Task:	
	
User	Compose an engaging travel blog post about a recent trip to this place, highlighting cultural experiences and must-see attractions.
SAISA	Title: Paradise Found: A Trip to the Hawaiian Islands Introduction: I recently had the opportunity to visit the beautiful Hawaiian Islands, and I must say, it was an unforgettable experience. The breathtaking views, crystal blue waters, and lush green landscapes truly make it a paradise on earth. In this blog post, I'll share some of my favorite moments and must-see attractions from my trip. Day 1: Arrival and Exploring Oahu Upon arrival, I was greeted by the stunning view of Waikiki Beach, which is located on the island of Oahu. I spent the day exploring the area, taking in the sights, and soaking up the sun. One of the highlights of my day was visiting the iconic Diamond Head, a volcanic crater that offers panoramic views of the beach and ocean. Day 2: Polynesian Cultural Center The next day, I visited the Polynesian Cultural Center, where I had the chance to experience the rich culture and traditions of various Polynesian islands. The center showcases traditional dances, music, and crafts, as well as interactive exhibits that allowed me to learn more about the history and customs of the region. Day 3: Hanauma Bay On my third day, I visited Hanauma Bay, a stunning natural wonder that is home to an abundance of marine life. The bay is a protected marine sanctuary, and visitors are required to take a guided tour to learn about the local ecosystem and conservation efforts. The crystal blue waters and vibrant coral reefs were truly breathtaking, and I was able to witness sea turtles, colorful fish, and other marine creatures up close. Day 4: Pearl Harbor and USS Arizona On my last day, I visited Pearl Harbor, the site of the infamous attack that led to the United States' entry into World War II. The USS Arizona Memorial is a must-see attraction, as it offers a solemn and educational experience. I was able to learn about the history of the attack and the significance of the USS Arizona in the war. Conclusion: In conclusion, my trip to the Hawaiian Islands was an unforgettable experience filled with cultural experiences, breathtaking views, and adventure. From the iconic Waikiki Beach to the protected marine sanctuary of Hanauma Bay, there is truly something for everyone to enjoy. I would highly recommend a visit to these beautiful islands for anyone looking to experience the wonders of nature and the rich history of the region.

Table 14: SAISA is capable of executing complex writing tasks based on a given image.